Available online at www.sciencedirect.com

ScienceDirect

Procedia Engineering 114 (2015) 70 – 77

Procedia Engineering

www.elsevier.com/locate/procedia

1st International Conference on Structural Integrity

Managing Welding Induced Distortion – Comparison of different computational approaches

Zuheir Barsoum[a,b]*, Mehdi Ghanadi[a,c], Shadi Balawi[b]

[a]*KTH Royal Institute of Technology, Department of Aeronautical & Vehicle Engineering, Teknikringen 8, 100 44, Stockholm, Sweden*
[b]*Khalifa University, Department of Aerospace Engineering, PO Box 127788, Abu Dhabi, United Arab Emirates*
[c]*Volvo Construction Equipment, Department of Virtual Product Development, Carl Lihnells road, 360 42, Braås, Sweden n*

Abstract

This study aims to assess and compare three different approaches of inherent strain method for prediction of welding induced distortion; inherent strain, inherent deformation and shrinkage force approaches. The FEA was performed on T-fillet welded structures. The results are compared with elastic-plastic FEA and experiments and shows a qualitative good agreement. It is found that the inherent strain and inherent deformation approaches are suitable to predict transverse shrinkage and transverse bending whereas to predict the longitudinal shrinkage and longitudinal bending the shrinkage force approach is more suitable.

Peer-review under responsibility of INEGI - Institute of Science and Innovation in Mechanical and Industrial Engineering

Keywords: computational weld mechanics; finite element analysis, welding distortion

1. Introduction

Accurate and reliable distortion predictions are essential for structural integrity of welded structures. However, finite element simulation of the welding process is highly non-linear and involves in general many phenomena e.g. non-linear temperature dependent material behavior, 3D nature of the weld pool and the welding processes and microstructural phase transformation. Distortion of a structure can be measured whilst in case of large complex structures it is expensive and also time consuming. Numerical analysis is then performed using finite element method that reduces the cost however in case of large welded structures, considering extremely nonlinear

---

* Corresponding author. Tel.: +46-70-230-4342; fax: +46-8- 790 91 30
E-mail address: zuheir@kth.se

Peer-review under responsibility of INEGI - Institute of Science and Innovation in Mechanical and Industrial Engineering
doi:10.1016/j.proeng.2015.08.043

mechanical behavior of welding, the computational expense are large and simplification linear finite element method have to be used. Fig. 1 illustrates different distortions that can occur after welding. An approach for distortion analysis is *inherent strain* where the plastic strain develops during the welding processes give rise to distortion. Inherent strain theory has been developed over the years [1-5] where most of the implementation of the method have been for the welded offshore and ship structures [6-7]. Other approaches for welding distortion analysis are *inherent deformation* and *shrinkage force* [8]. This study aims to assess and compare three different approaches of inherent strain method for prediction of welding induced distortion; inherent strain, inherent deformation and shrinkage force approaches. The FEA was performed on T-fillet welded structures. The analysis is also performed with thermo elastic-plastic FEA using the welding simulation approaches developed by the authors [9-11].

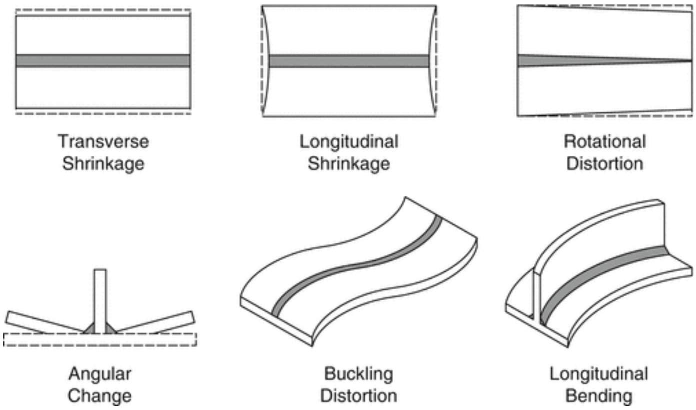

Fig. 1. Classification of welding distortion.

2. Specimens and experimental set up

The specimen used for distortion measurement was a T-fillet joint made of S355 steel, both for the base and filler material. The dimensions and boundary conditions during welding are shown in fig. 2a. During welding, the baseplate has been clamped in one side and in 60 mm from center of the baseplate. Fig 2b shows the set up for measurement of the welding deformation using a Wenzel LH1512. By setting the moving coordinate system, the measuring device is moved on the surface of the specimen and measures the deformation of some specified points both on baseplate and stiffener. Tab. 1 presents the welding parameters used.

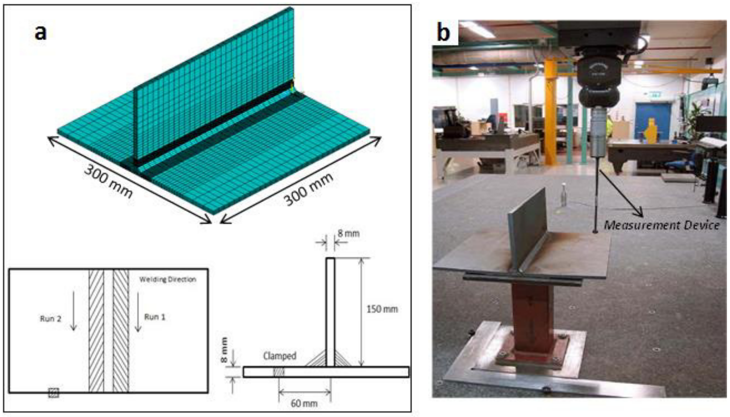

Fig. 2. (a)T-Fillet joint, geometry an mesh; (b) experimental set up and measurement.

Table 1. Welding parameters

Throat thickness (mm)	Current (I)	Voltage (V)	Weld length (mm)	Welding speed (mm/s)	Weld passes
4	390	30	6	13.3	1

3. Nonlinear finite element analysis

The finite element software *ANSYS v.13* has been used to carry out the nonlinear elastic-plastic finite element analysis for the welding simulation. Weld bead is modeled with the base plate and stiffener and all represent a single geometry. The weld bead is divided into adequate number of volumes (blocks) which will be used in the implementation of the moving heat source and rapid dumping approach. The simulations are carried out sequentially; thermal analysis in order to obtain the temperature distributions and the sub-sequent elastic-plastic nonlinear mechanical analysis. The temperature dependent thermo-mechanical properties for S355 steel is taken from [9]. The details about the finite element procedure for welding simulation developed previously are found in [9-11].

3.1. Inherent strain zone

The inherent strain region which is determined through the non-linear FEA is the residual plastic strain created due plastic deformation during the welding. This is determined by the average value of the inherent strain distribution along the weld line. Fig. 3 shows the inherent strain distribution in the mid cross section of the T-fillet joint. The plastic zone along the plate width is narrowed to where the weld joint and most of the plastic deformation occurs, approximately in a region of 40 mm. Beyond this region no plastic/inherent strain is observed. However, the inherent strain will vary along the welding line due to the 3D nature of welding and moving heat source; plastic deformation will occur subsequently as the heat source travels along the weld line. A good approximation is that the inherent strain is evenly distributed and averaged.

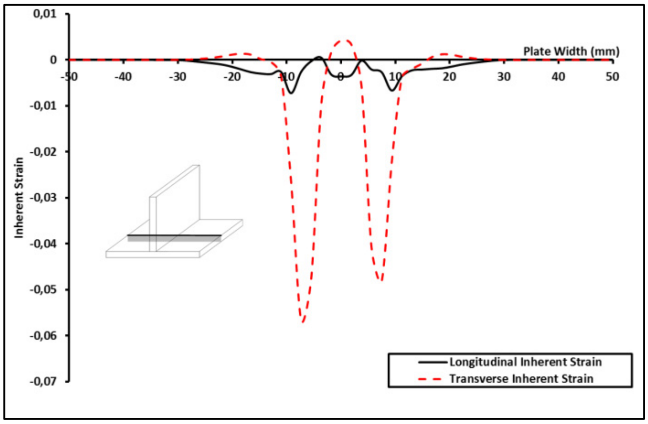

Fig. 3. Inherent strain distribution in T-fillet weld.

4. Elastic finite element analysis

Elastic FEA may be used to predict the welding distortion when the inherent strain region and averaged magnitude is known for the particular joint. Different inherent approaches exists which are based on different initial conditions; how you apply the inherent parameter. In *inherent strain* approach, the inherent strains components are directly applied on the inherent strain zone and the elastic FEM analysis is carried out. In other approaches the inherent strain is integrated over the welding line then the results in the form of displacements and forces, *inherent deformation* and *shrinkage force*, are applied on the inherent strain zone.

4.1. Inherent strain approach

The longitudinal and transverse inherent strain is calculated by elastic plastic analysis. As a good approximation, the average value of inherent strain distribution is calculated along the welding line and then the result is considered as inherent strain zone, fig. 3. The magnitude of the inherent strain, ε, consists of bending (ε^b) and membrane (ε^m) strain components, eq. 1. The inherent strain components are integrated over thickness (t) and the results applies on each element in the inherent strain zone, eq. 2, and assuming constant inherent strain. In this sense, the in-plane and bending items causes in plane strain and curvature respectively

$$\boldsymbol{\varepsilon = \varepsilon^m + \varepsilon^b} \qquad (1)$$

$$\boldsymbol{\varepsilon^m = \frac{1}{t}\int_{\frac{-t}{2}}^{\frac{t}{2}} \varepsilon dy} \qquad (2)$$

4.2. Inherent strain approach

The inherent deformation is calculated by integration of inherent strain over the cross section of the plate and perpendicular to welding line. The inherent deformation may be divided into four components: longitudinal shrinkage (δ_L^*), transverse shrinkage (δ_T^*), longitudinal bending (θ_L^*), and transverse bending (θ_T^*), where defined by the following equations:

$$\boldsymbol{\delta_z^* = \frac{1}{t}\iint \varepsilon_z^*\, d_x d_y} \qquad (3)$$

$$\boldsymbol{\delta_x^* = \frac{1}{t}\iint \varepsilon_x^*\, d_x d_y} \qquad (4)$$

$$\boldsymbol{\theta_z^* = \frac{1}{I}\iint t\varepsilon_z^*\, d_x d_y} \qquad (5)$$

$$\boldsymbol{\theta_x^* = \frac{1}{I}\iint t\varepsilon_x^*\, d_x d_y} \qquad (6)$$

Moment of inertia, *I*, is defined as:

$$I = \frac{1}{12}\iint t^2 d_x d_y \qquad (7)$$

The average value of inherent deformation components along welding length (L_W) , is calculated by below equations and the averaged inherent deformations as initial displacements are applied on the inherent strain zone in the elastic FE model:

$$\boldsymbol{\bar{\delta}_z^* = \frac{1}{L_W}\int_0^L \delta_z^*\, dz} \qquad (8)$$

$$\boldsymbol{\bar{\delta}_x^* = \frac{1}{L_W}\int_0^L \delta_x^*\, dz} \qquad (9)$$

$$\boldsymbol{\bar{\theta}_z^* = \frac{1}{L_W}\int_0^L \theta_z^*\, dz} \qquad (10)$$

$$\overline{\boldsymbol{\theta}}_x^* = \frac{\mathbf{1}}{\boldsymbol{L_w}} \int_0^L \boldsymbol{\theta}_x^*\, \boldsymbol{dz} \quad (11)$$

The length of the T-joint structures is divided by 30 sections on each side. The inherent deformation and inherent bending are illustrated in fig 4. The inherent deformation components are calculated on each cross section along the welding line. Average values are then calculated and shown as straight lines. In order to remove the side effect errors, the points that are closed to edges are neglected. In this case, both baseplate and stiffener are analyzed. It can be seen that the average value of inherent components are almost the same for both sides of weld center line.

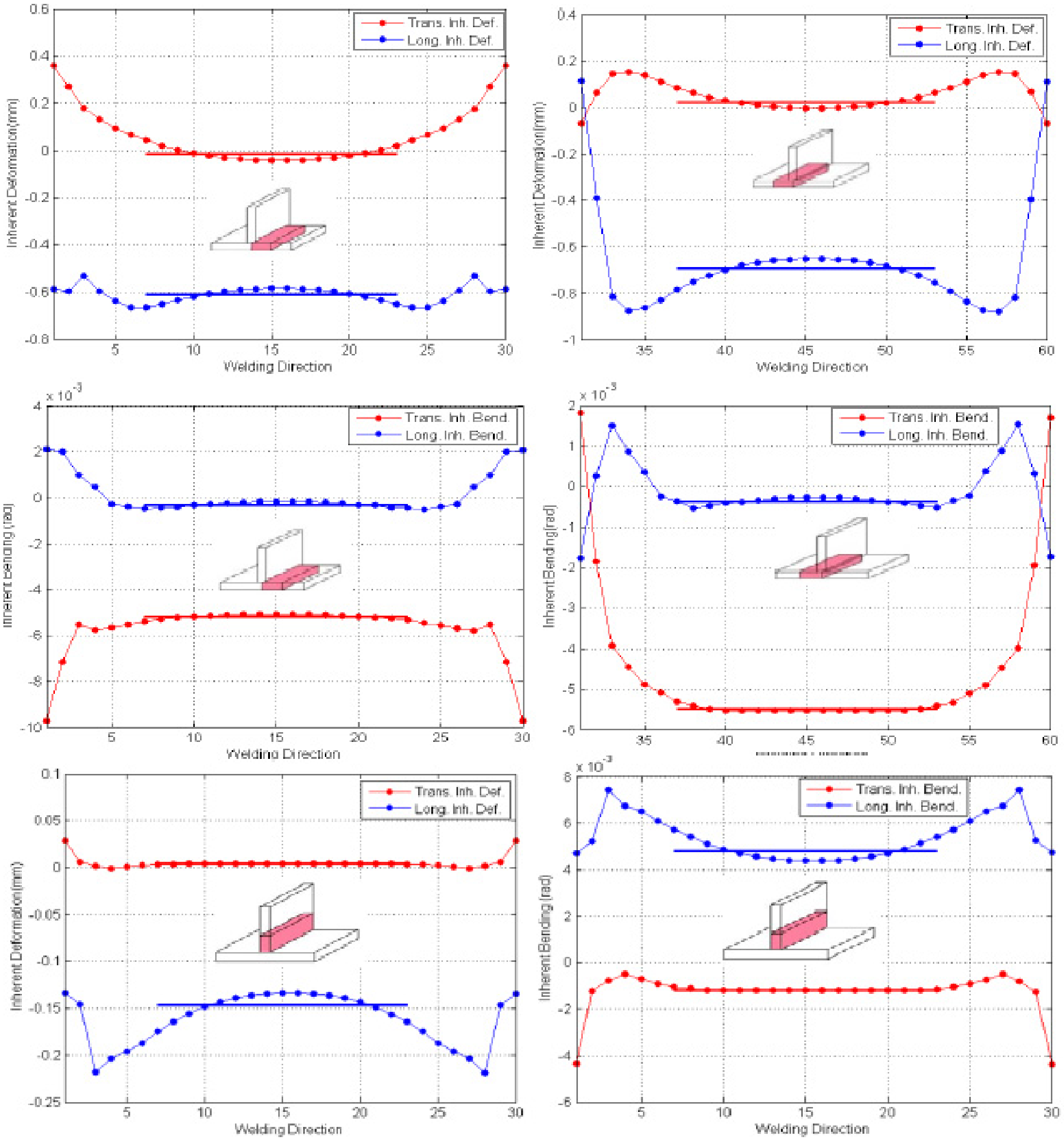

Fig. 4. Inherent deformation and bending in baseplate and stiffener.

4.3. Shrinkage force approach

Welding distortion can also be calculated by applying equivalent force and moments. Using the following equations, the longitudinal and transverse inherent strains are integrated over cross section of the welding line.

$$\boldsymbol{F_z^* = E \int \varepsilon_z^* dxdy} \quad (1)$$

$$\boldsymbol{F_x^* = E \int \varepsilon_x^* dxdy} \quad (2)$$

$$\boldsymbol{M_z^* = EI\theta_z^*} \quad (3)$$

$$\boldsymbol{M_x^* = EI\theta_x^*} \quad (4)$$

The longitudinal shrinkage force (F_z) and longitudinal moment (M_z) are applied on inherent strain zone. Since the analysis is performed on flat plates, then the transverse shrinkage force (F_x) and transverse moment (M_x) are applied on the nodes located at both ends of the plate. In order to get the loading per node, the force should be divided by the number of nodes that exists in inherent strain zone .Thereafter the nodal load has to be applied on each node and then carry out elastic analysis. Fig 6 illustrates how the shrinkage forces and moments are distributed in a plate. Fig 6 shows the distribution of the shrinkage force in the T-fillet joints baseplate.

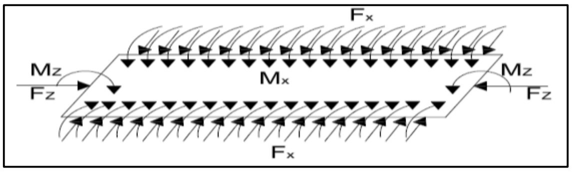

Fig. 5. Distribution of shrinkage forces an moments.

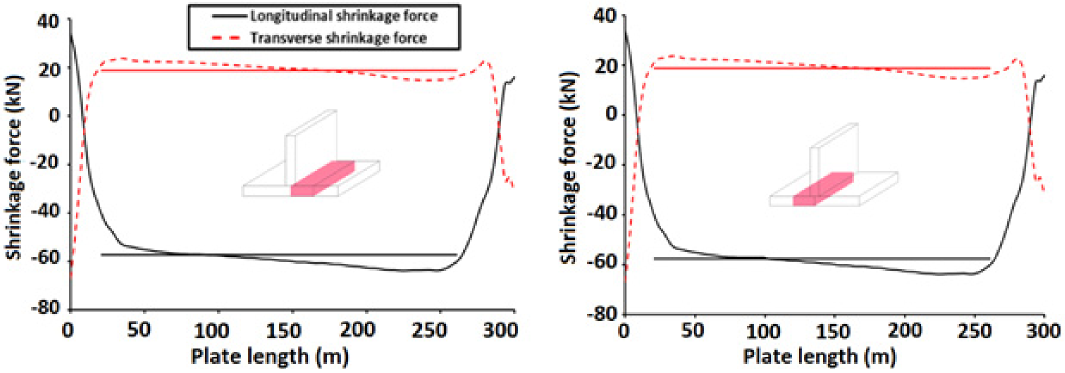

Fig. 6. Shrinkage force distribution in T-fillet joint.

5. Comparison of different approaches

Distortion components calculated by three inherent strain based methods are compared in fig. 7, which shows the maximum out of plane deformation, also compared with measurements. It is observed, considering the constraint conditions, the maximum transverse bending occurs in front edge of the model. For the T-joint the maximum longitudinal bending occurs at the side edge that corresponds to constraint conditions. Tab. 2 shows the other two deformation components; longitudinal and transverse shrinkages. The results are also compared with elastic-plastic analysis and experimental data.

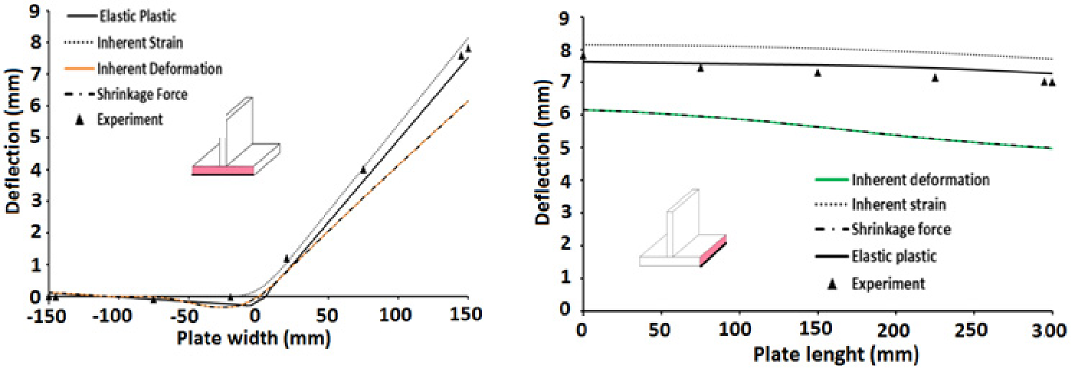

Fig. 7. Distortion prediction using the elastic-plastic analysis, inherent concepts and experiments.

Table 2. Comparison of maximum distortion using different methods

	Elastic-Plastic FEM	Elastic FEM		
		Inherent strain	Inherent deformation	Shrinkage force
Longitudinal shrinkage (mm)	-0.31	-0.5	-0.4	-0.4
Transverse shrinkage (mm)	-0.1	0.25	-0.12	-0.16
Angular distortion (mm)	0.051	0.052	0.041	0.041

6. Conclusions

Distortion analysis can be carried out using full nonlinear/elastic-plastic welding simulation or elastic FEA adopting one of the inherent strain approaches. The full elastic plastic analysis requires large computational time due to e.g. nonlinear material properties. For the fairly simple welded T-joint the CPU time was approximately 5 hours for the 3D analysis. In distortion analysis using elastic FE models the CPU time is less than 1 minute.

The determination of the inherent strain distribution is essential in order to carry out the elastic FEA. From this inherent strain distribution it is possible to identify the average value of the inherent strain zone along the welding line where the averaged inherent strain value will serve as the initial condition in such analysis. The longitudinal and transverse inherent strain distributions shows the maximum inherent strain zone in the middle cross section of the T-joint, where maximum thermal gradient have occurred. However, large variation is observed in the start and stop position of the welding, i.e. edge effects. Thus, the average value of the inherent deformation should be calculated by neglecting the results from the nodes and elements locate near the plate edges.

In fig. 5 the out of plane deformations are compared using the different distortion analysis concepts with elastic plastic FEM and measurements. It can be observed that the inherent strain predicts the distortion with good accuracy as compared with the other approaches. The inherent deformation and shrinkage force requires an integration step, which will result in a poorer distortion approximation. The bending deformation will have an effect on the angular distortion, which is a more influential on the out of plane deformation than longitudinal and transverse shrinkages. . It is found that the inherent strain and inherent deformation approaches are suitable to predict transverse shrinkage and transverse bending whereas to predict the longitudinal shrinkage and longitudinal bending the shrinkage force approach is more suitable.

References

[1] Martin Birk Sorensen ,‘Simulation of welding distortions in ship section’, Industrial PHD ,Odense Steel Shipyard LTd.,1999,department of naval architecture and offshore engineering

[2]T.L.Teng, C.Fung, P.Chang, W.Yang , 2001, ”Analysis of residual stresses and distortions in T-joint fillet welds”, Pressure Vessels and Piping J., Vol.78, pp.523-538.

[3] Artem Pilipenko, ‘Computer simulation of residual stress and distortion of thick plates in multi-electrode submerged arc welding. their mitigation techniques’, phd thesis, department of machine design and materials technology norwegian university of science and technology, norway,2011.

[5] Yu LUO, Hidekazu Murakawa, Yukio Udea, 1997*,* ” Prediction of Welding Deformation and Residual Stress by Elastic FEM Based on Inherent Strain(Report I)-Mechanism of Inherent Strain Production”, Transactions of JWRI, Osaka University, Ibaraki, Osaka,Japan.

[6]D.Deng, Hidekazu Murakawa, Masakazu Shibahara, 1989, ”Investigations on welding distortion in an asymmetrical curved block by means of numerical simulation technology and experimental method ”, Computational Materials Sience J., Vol.48,2010, pp.187-194.

[7] Madhu S Nair,Hidekazu Murakawa , ”Theoretical study of forming of twisted T-section longitudinal investigation from aspect of inherent strain (1st report)”,J.Kansai SOC. N.A, Japan No.237, March 2002.

[8]Adan Vega Saenz, ”Development of inherent deformation database for automatic forming of thick steel plates by line heating considering complex heating patterns”, Doctoral Thesis, Osaka University, Japan.

[9] Bhatti A. A. and Barsoum Z. Development of efficient 3D welding simulation approach for residual stress estimation in different welded joints. J of Strain Anal 2012; 47/8: 539-552.

[10] Bhatti A.A., Barsoum Z., Murakawa H. and Barsoum I. Influence of thermo-mechanical material properties of different steel grades on welding residual stresses and angular distortion. J of Materials & Design, 2015; 65: 878–889.

[11] Bhatti A. A., Barsoum Z. and Khurshid M. Development of FE simulation framework for prediction of residual stresses in large welded structures. Computers & Structures. 2014; 133: 1-11.